Original Article
An engineered FGF21 variant, LY2405319, can prevent non-alcoholic steatohepatitis by enhancing hepatic mitochondrial function

Ju Hee Lee[1,2*], Yea Eun Kang[2*], Joon Young Chang[2,3], Ki Cheol Park[4], Hyeon-Woo Kim[2,3], Jung Tae Kim[2,3], Hyun Jin Kim[1,2], Hyon-Seung Yi[2], Minho Shong[1,2], Hyo Kyun Chung[2], Koon Soon Kim[1,2]

[1]Department of Internal Medicine, Chungnam National University Hospital, Daejeon 35015, Republic of Korea; [2]Research Center for Endocrine and Metabolic Diseases, Chungnam National University School of Medicine, Daejeon 35015, Republic of Korea; [3]Department of Medical Science, Chungnam National University School of Medicine, Daejeon 35015, Republic of Korea; [4]Clinical Research Institute, Daejeon St. Mary's Hospital, College of Medicine, The Catholic University of Korea, Daejeon 34943, Republic of Korea. *Equal contributors.

Abstract: Non-alcoholic fatty liver disease (NAFLD) is a prevalent obesity-related disease that affects large populations throughout the world due to excessive calorie intake and an increasingly sedentary lifestyle. Fibroblast growth factor 21 (FGF21) has recently emerged as a promising therapeutic candidate for the treatment of obesity and diabetes. FGF21 is a starvation-induced pleiotropic hormone with various beneficial metabolic effects, and pharmacological treatment in rodents has been shown to improve insulin sensitivity and decrease simple fatty liver disease. However, its effects on reversing the symptoms of advanced liver disease have yet to be validated. Here, we investigated the protective effects of the LY2405319 compound, an engineered FGF21 variant, in a non-alcoholic steatohepatitis (NASH) model using *leptin*-deficient *ob/ob* mice and a methionine- and choline-deficient (MCD) diet to induce steatohepatitis. LY2405319 treatment in *ob/ob* mice corroborated previous results showing that improvements in the metabolic parameters were due to increased mitochondrial oxygen consumption rate and fatty acid oxidation. LY2405319 treatment in *ob/ob* mice on an MCD diet significantly reduced the symptoms of steatohepatitis, as confirmed by Masson's trichrome staining intensity. Serum levels of AST and ALT were also reduced, suggesting an attenuation of liver injury, while detection of inflammatory markers showed decreased mRNA expression of TGF-β1 and type-I collagen, and decreased phosphorylation of NF-kB p65, JNK1/2, and p38. Collectively, these data show that LY2405319 treatment attenuated MCD diet-induced NASH progression. We propose that the LY2405319 compound is a potential therapeutic candidate for the treatment of advanced liver disease.

Keywords: LY2405319, FGF21, non-alcoholic fatty liver disease, non-alcoholic steatohepatitis, mitochondria, inflammation

Introduction

Non-alcoholic fatty liver disease (NAFLD) is the most common liver disease in many parts of the world [1, 2]. NAFLD encompasses a spectrum of liver pathologies with different clinical manifestations, from the simple accumulation of triglycerides within hepatocytes to steatohepatitis, cirrhosis, and primary liver cancer [3-5]. Several hypotheses have been proposed regarding the pathogenesis of NAFLD, from a "double hit" model to a "multi-hit" model, which involves lipotoxicity, oxidative stress, endoplasmic reticulum stress, chronic inflammatory stress and mitochondrial dysfunction [6, 7]. In both hypotheses, insulin resistance is regarded as the key pathogenic factor of NAFLD, suggesting that NAFLD is a manifestation of metabolic syndrome [8, 9]. Consequently, metformin and thiazolidinedione have been introduced as treatments for NAFLD, with modest benefits. Nevertheless, effective therapeutic drugs focusing on the liver pathophysiology have not been developed.

Fibroblast growth factor 21 (FGF21) is a circulating protein with pleiotropic metabolic actions [10]. Physiologically, FGF21 expression is induc-

ed in the liver by prolonged fasting and in white adipose tissue by feeding [11, 12]. In mouse models of diabetes and obesity, pharmacological administration of FGF21 normalized plasma glucose levels, improved insulin sensitivity, reduced plasma triglyceride and cholesterol levels, reversed hepatic steatosis, and increased energy expenditure [13-15]. Furthermore, similar beneficial effects were observed in non-human primates and obese humans with type 2 diabetes [16, 17]. These findings support its development as a novel therapy for the treatment of NAFLD and other metabolic disorders [18]. However, the mechanism of FGF21 action in NAFLD has not been fully addressed. White adipose tissue expresses high levels of fibroblast growth factor receptor 1 and β-klotho and is considered the predominant site of FGF21 action, suggesting that the beneficial effects of FGF21 *in vivo* may result, in part, from its direct effects on adipose tissue [19]. However, Fisher et al. showed that FGF21 activated signaling and transcriptional events within the liver and peripheral tissues [20]. Therefore, a direct effect of FGF21 on the liver cannot be ruled out [21].

LY2405319 is an engineered FGF21 protein with a disulfide bridge (L118C-A134C) in the C-terminus and a S167A substitution to improve the conformational stability and productivity of the recombinant protein, respectively [22]. LY2405319 is indistinguishable from native human FGF21 in cell-based, rodent, and non-human primate studies with respect to potency, selectivity, biological activity and efficacy. In a clinical trial, LY2405319 significantly reduced body weights, fasting insulin levels, fasting triglycerides, and total and low density lipoprotein cholesterol levels and robustly increased serum adiponectin and high density lipoprotein cholesterol levels [17]. However, the therapeutic effects of either native FGF21 or LY2405319 on NAFLD have only been reported as reducing hepatic steatosis. The reversal of steatohepatitis, fibrosis, and hepatic steatosis needs to be confirmed for LY2495319 to be an attractive therapeutic modality for NAFLD.

In this study, we reported that the pharmacological effects of LY2405319 on non-alcoholic steatohepatitis (NASH) were to improve hepatic steatosis, reduce inflammation, and reverse fibrosis in the liver. Furthermore, we found that LY2405319 directly restored mitochondrial function in primary hepatocytes cultured from the experimental model.

Materials and methods

Animals and treatments

All experimental procedures were completed in accordance with the Institutional Animal Care and Use Committee of the Chungnam National University School of Medicine (Daejeon, South Korea). Six-week-old male *ob/+*control mice and *ob/ob* C57BL/6J Lep[(-/-)] mice were purchased from Harlan (Indianapolis, IN, USA). These mice were maintained under standard conditions (22°C and 12-h light/dark cycle) and fed a normal chow diet. The mice were divided into three groups (n = 10 each group), including the *ob/+*control, vehicle-treated (*ob/ob*-Vehicle) and LY2405319-treated groups (*ob/ob*-LY), to test the therapeutic effects of LY2405319 (Eli Lilly Indianapolis, IN, USA) on the livers of *ob/ob* mice. LY2405319 was provided by Eli Lilly and Co. and generated as previously described [22]. *ob/ob* mice were intraperitoneally administered vehicle or LY2405319 (5 mg/kg) for 3 weeks. Body weights were recorded every 5 days during the experimental period. For the fibrosis studies, 6-week-old male *ob/ob* mice were fed either a methionine- and choline-deficient (MCD) diet (#A02082002B; Research Diets, Inc., New Brunswick, NJ, USA) or a control diet for 4 weeks. *ob/ob* mice were divided into a control group that was fed a normal chow diet (*ob/ob*-vehicle) and an MCD group that was fed the MCD diet plus vehicle (*ob/ob*-MCD-vehicle) or LY2405319 (*ob/ob*-MCD-LY; 5 mg/kg) for 4 weeks. Body weights were recorded at the start and end of the experimental period. Liver aliquots were snap frozen in liquid nitrogen and stored at -80°C until analysis. A portion of each liver was fixed in 10% neutral formalin for histology.

Intraperitoneal glucose tolerance and insulin tolerance tests

For the intraperitoneal glucose tolerance test (IPGTT), mice were fasted for 16 h and then 2 g/kg or 1 g/kg glucose was injected into the intraperitoneal cavity of each mouse. Blood glucose levels were measured at 0, 15, 30, 60, 90 and 120 min using a glucometer (ACCU-CHEK, Roche Diagnostics Corporation, IN). The intraperitoneal insulin tolerance test (IPITT)
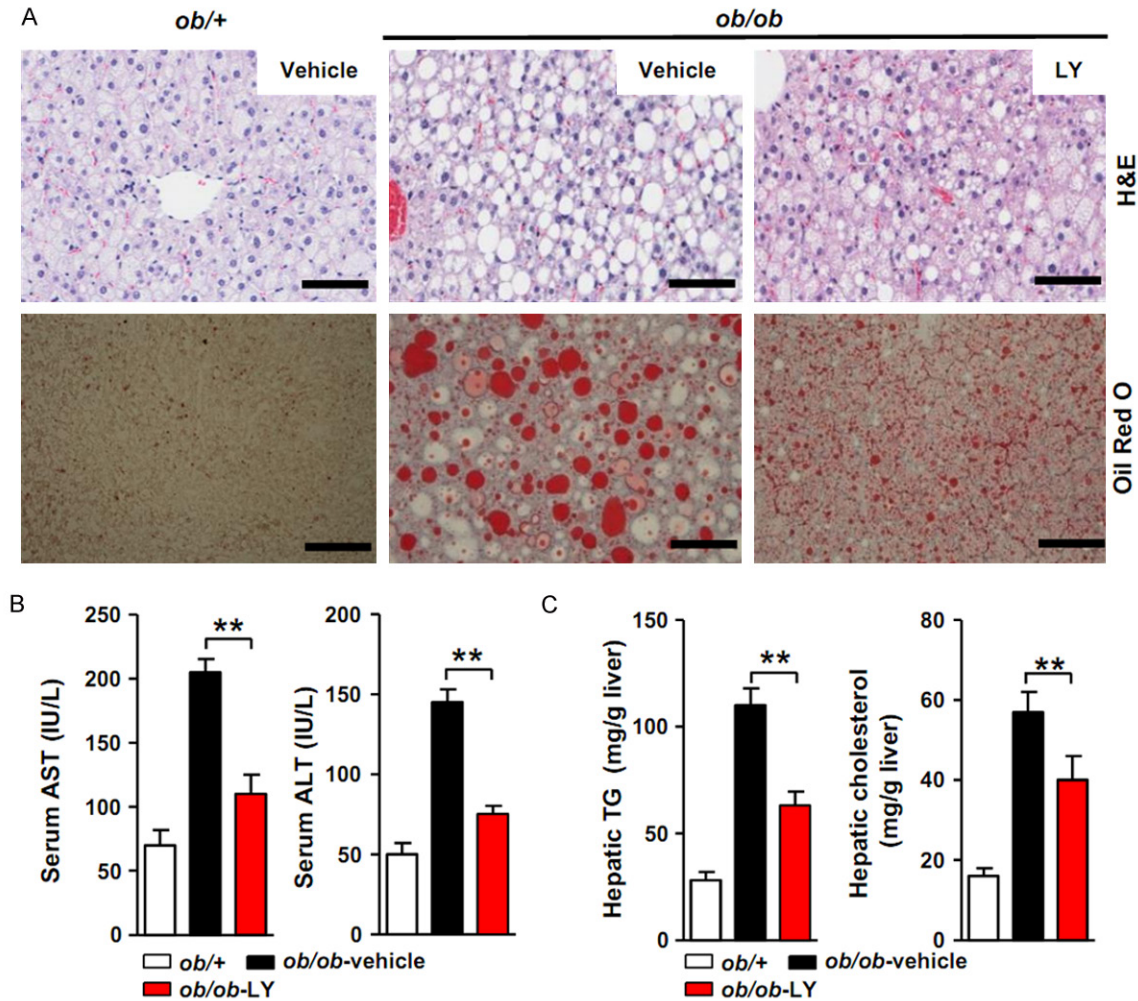
Figure 1. Effect of the LY2405319 treatment on hepatic steatosis in *ob/ob* mice. (A) Hepatic steatosis was evaluated with H&E and Oil Red O staining. Vehicle or LY2405319 (5 mg/kg) was administered to *ob/ob* mice by IP injection for 3 weeks. H&E and Oil Red O staining of the livers showed a marked improvement of steatosis. Vehicle vs. LY2405319. Magnification 400×. (B) The serum AST and ALT levels were reduced in the LY2405319 group compared with the vehicle group. **$P < 0.01$. Vehicle vs. LY2405319 (n = 10 per group). (C) Hepatic TG and cholesterol levels were significantly reduced in the LY2405319 group compared with the vehicle group (n = 10 per group). All data are presented as the mean ± sem, **$P < 0.01$.

was performed by measuring the blood glucose levels after a 6 h fast, followed by an intraperitoneal insulin injection (0.75 U/kg; Humalog).

Indirect calorimetry

Mice were fed standard chow and placed into individual metabolic chambers, with free access to food and water. Oxygen consumption (VO_2), carbon dioxide production (VCO_2) and energy expenditure (EE) were measured using a Physical cage system (Oxylet, Panlab, Cornella, Spain). The data were analyzed using METABOLISM software version 2.2. The average values obtained during the light and dark

periods were calculated. Student's *t*-test was used to calculate the *p* values.

Serum analysis

Blood was collected from the heart under general anesthesia. The blood was centrifuged at 10,000 rpm for 5 min, and the supernatant was collected. Serum levels of aspartate aminotransferase (AST), alanine aminotransferase (ALT), triglyceride (TG) and total cholesterol were measured using a Hitachi 7180 autoanalyzer and Wako reagents (Wako Pure Chemical Industries, Osaka, Japan). Serum and hepatic tumor necrosis factor-α (TNF-α) levels were

measured using ELISA kits (R&D Systems, Minneapolis, MN).

Assessment of liver histology and immunohistochemistry

The livers were fixed in 10% (v/v) neutral formalin and embedded in paraffin to evaluate steatosis and inflammation. Four micrometer-thick sections were cut and stained with hematoxylin-eosin (H&E) and Masson's trichrome. For the detection of neutral lipids, 10 um-thick cryosections were stained with 0.5% (v/v) Oil Red O for 60 min at room temperature and then counterstained with hematoxylin. Immunohistochemistry of paraffin-embedded liver sections was performed using an anti-8-OHdG antibody (#ab62623, Abcam) to characterize oxidative damage. For the immunohistochemical analysis, the liver sections were incubated with a primary anti-F4/80 antibody (#ab6640, Abcam), followed by incubation with the corresponding secondary antibody. Positive staining was detected using a 3,3'-Diamin-obenzidine (DAB) Kit (Dako, Ely, Cambridgeshire, UK). Images were acquired at 200× or 400× magnification, and the percentage of the positively stained area was analyzed.

Analysis of thiobarbituric acid-reactive substances (TBARS)

Lipid peroxidation in liver tissues was analyzed by measuring the levels of thiobarbituric acid-reactive substances (TBARS) using a commercial TBARS assay kit (Cayman Chemical, Ann Arbor, MI, USA), according to the manufacturer's specifications. Briefly, after treatment, the liver tissue was suspended in RIPA buffer, sonicated and then centrifuged at 2,000×g for 10 min at 4°C. Supernatants were collected, added to sodium dodecyl sulfate, mixed with the color reagent, and boiled for 30 min. The TBARS levels were quantified spectrophotometrically using a plate reader, and the results were normalized to the protein concentrations.

Measurement of the oxygen consumption rate (OCR)

The oxygen consumption rate was measured in 24-well plates using a Seahorse XF24 analyzer (Seahorse Bioscience Inc., North Billerica, MA, USA) as previously described [23]. The cells were seeded at a density of 20,000-50,000 cells per well 18 h prior to the analysis. The day

before the OCR measurement, the sensor cartridge was calibrated with calibration buffer at 37°C in a non-CO$_2$ incubator. Immediately before the measurement, the cells were washed and incubated with media lacking sodium bicarbonate at 37°C. Three readings were taken after the addition of each mitochondrial inhibitor, but before the injection of the subsequent inhibitor. Oligomycin (2 μg/ml), carbonylcyanide m-chlorophenyl hydrazine (CCCP, 5 μM) and rotenone (2 μM) were used as the mitochondrial inhibitors. The OCR was automatically calculated and recorded by the sensor cartridge and Seahorse XF-24 software.

Isolation of primary hepatocytes

Mouse primary hepatocytes were prepared from 8-week-old male C57BL/6J mice using the collagenase (0.8 mg/ml) perfusion method [24]. Isolated cells were further purified by a Percoll density gradient and plated at an appropriate density in Medium 199 (Sigma-Aldrich, St. Louis, MO, USA) in culture plates. After the cells were allowed for attach for 3-6 h, the medium was changed to remove unattached cells. All cells were tested for mycoplasma contamination using the MycoAlert PLUS mycoplasma detection kit (Lonza, Basel, Switzerland).

Western blot analysis

Western blot analysis was performed using standard methods with commercially available antibodies. Anti-phospho-NF-κB p65 (#3039), anti-phospho-JNK1/2 (#9255), anti-phospho-p38 MAPK T180/Y182 (#9211), anti-p38 MAPK (#9212) and anti-GAPDH (#2118) antibodies were obtained from Cell Signaling Technology. Secondary antibodies (goat anti-mouse and goat anti-rabbit) were obtained from Cell Signaling Technology (Beverley, MA, USA). The images were scanned using ODYSSEY and quantified using the Image Studio Digits software (LI-COR Biosciences, NE).

RNA isolation and analysis by quantitative Real-Time PCR (qRT-PCR)

RNA isolation and qRT-PCR were performed as previously described [24]. Briefly, total RNA was prepared using TRIzol reagent, and cDNAs were synthesized from the total RNA using M-MLV reverse transcriptase (invitrogen). The resulting cDNAs were amplified using the 7500 Fast
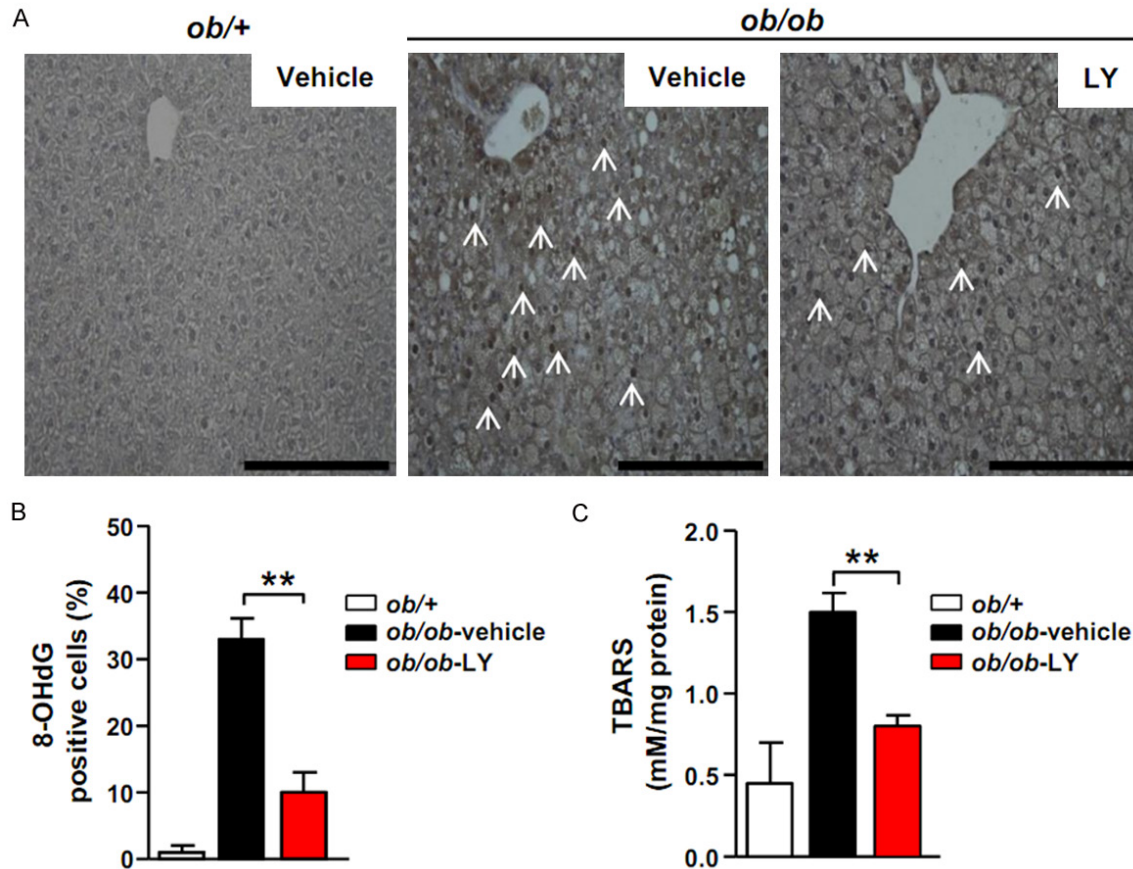
Figure 2. LY2405319 prevents oxidative stress and lipid peroxidation. (A) Immunohistochemical analysis of 8-OHdG in the livers of *ob/*+control, vehicle- and LY2405319-treated *ob/ob* mice. The arrows indicate 8-OHdG-positive cells. Magnification, 400×. (B) 8-OHdG expression in the livers of *ob/*+control, vehicle- and LY2405319-treated *ob/ob* mice (n = 10 per group). **$P < 0.01$. (C) Lipid peroxidation was determined by assaying the TBARS content in liver homogenates from *ob/*+control, vehicle- and LY2405319-treated *ob/ob* mice. All data are presented as the mean ± sem, **$P < 0.01$.

Real-Time PCR System and software (Applied Biosystems, Foster City, CA). Real-time PCR was performed in triplicate with individual time-matched vehicle-treated or control mice using 2× SYBR Green Mix (Applied Biosystems). All quantitative calculations were performed using the dCT method and normalized to GAPDH. The primer sequences were: *Tnf-α*: 5'-AGCACAGAAA-GCATGATCCG-3' and 5'-GCCACAAGCAGGAATG-AGAA-3'; *Collagen 1a*: 5'-ATGTTCAGCTTTGTG-GACCTC-3' and 5'-TCCCTCGACTCCTACATCTTC-3'; TGF-β1: 5'-CAACATGTGGAACTCTACCA-3' and 5'-GTATTCCGTCTC-CTTGGTTC-3'; and *Gapdh*: 5'-GA-CATGCCGCCTGGAGAAAC-3' and 5'-AGCCCAGGA TGCCCTTTAGT-3'.

Statistical analysis

Statistical analyses were performed using Stat Graph Prism (5.0) (GraphPad; San Diego, CA,

USA). The data are reported as the mean ± standard error of the mean (SEM). A two-tailed Student's t-test was used to determine differences between the groups. One-way analysis of variance was used to evaluate differences between groups with appropriate post hoc tests. Statistical significance was set at a *P* value of less than 0.05.

Results

An engineered FGF21 variant, LY2405319, reversed hepatic steatosis in ob/ob mice

We intraperitoneally administered LY2405319 (5 mg/kg) or vehicle to 6-week-old male *ob/ob* mice for 3 weeks to verify the improvement in NAFLD by LY2405319. Compared with the livers of *ob/*+control mice, the livers of *ob/ob* mice showed an accumulation of micro- and
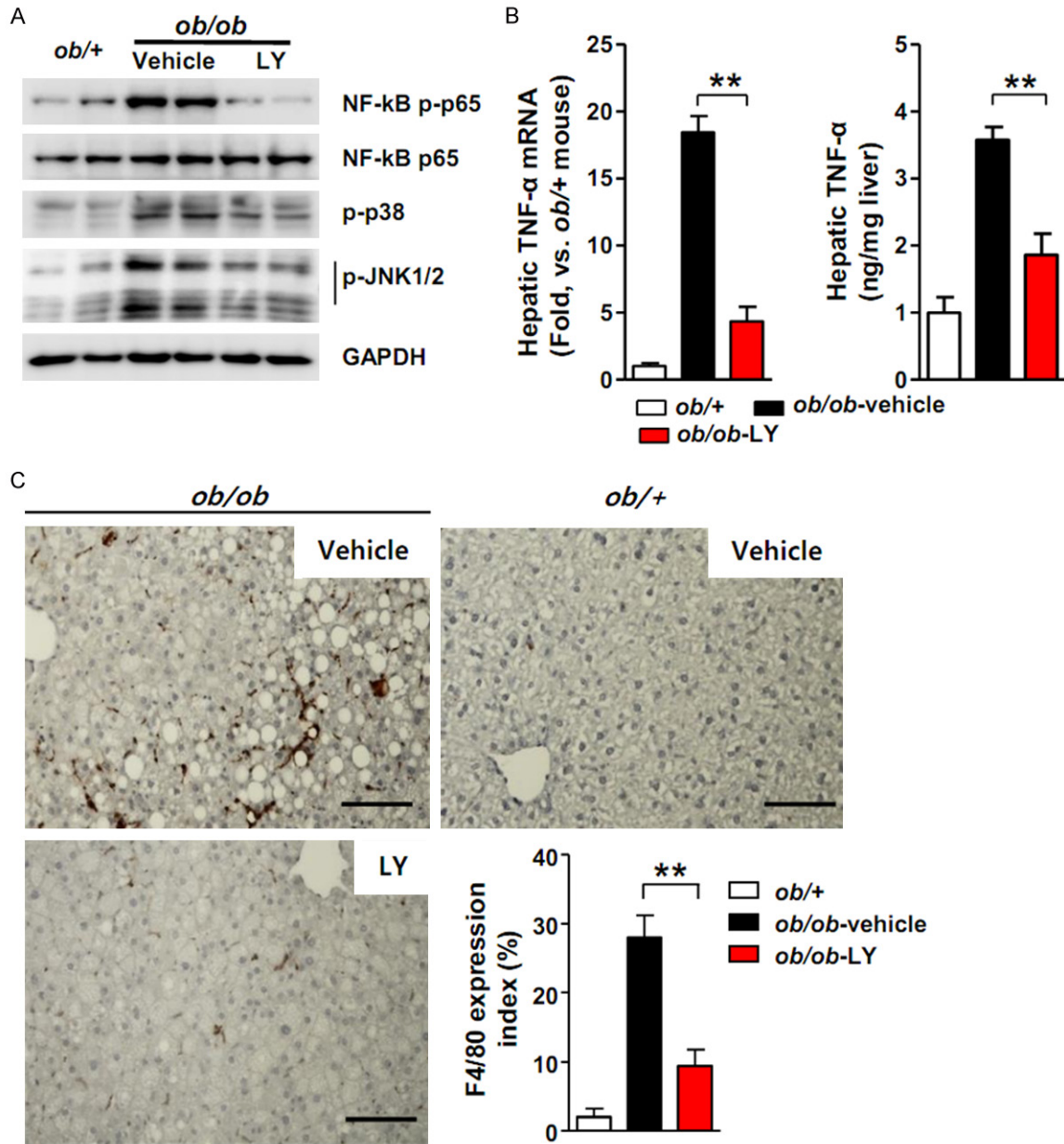
Figure 3. LY2405319 decreases inflammatory signaling and macrophage infiltration in *ob/ob* mouse livers. (A) Effect of LY2405319 on inflammatory signaling in the livers of *ob/ob* mice treated with or without LY2405319. Western blots were performed on liver extracts to detect NF-kB p65, p38 MAPK and JNK 1/2 phosphorylation. The blots are representative of three independent experiments. (B) Hepatic TNF-α mRNA and serum TNF-α levels in *ob/+*control and *ob/ob* mice treated with or without LY2405319. (n = 7-9 per group). **$P < 0.01$. Vehicle vs. LY2405319. (C) Immunohistochemistry with an anti-F4/80 macrophage-specific antibody in the livers of vehicle- or LY2405319-treated *ob/ob* mice. **$P < 0.01$. Vehicle vs. LY2405319, (n = 7-9 per group). Magnification, 400X. All data are presented as the mean ± sem, **$P < 0.01$.

macrovesicular intracytoplasmic fat droplets in liver parenchymal cells. H&E staining of the liver sections showed that hepatic steatosis was substantially attenuated in *ob/ob* mice following the systemic administration of LY-2405319 (**Figure 1A**). In addition, lipid droplets confirmed by Oil Red O staining were reduced in the livers of LY2405319-treated *ob/ob* mice compared with vehicle-treated *ob/ob* mice. This change was accompanied by a marked reduction in the serum levels of the liver injury markers AST and ALT (**Figure 1B**). The hepatic triglyceride and cholesterol levels were also significantly decreased in the LY2405139-treated
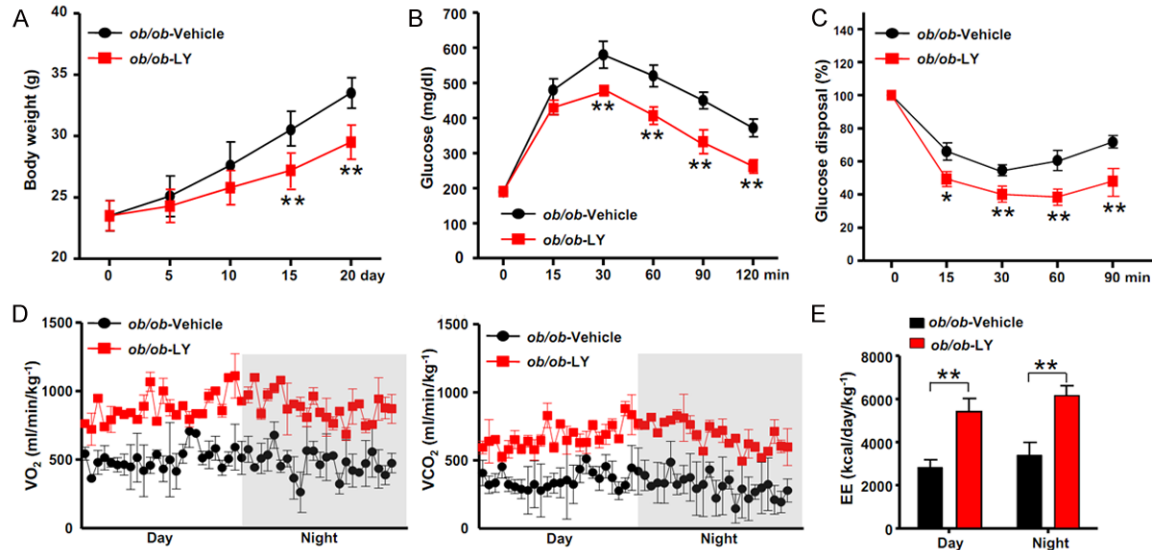
Figure 4. LY2405319 improves the metabolic parameters. (A) Body weights of *ob/ob* mice treated with or without LY2405319 (n = 10 per group). (B) IPGTT. At 9 weeks of age, mice were fasted overnight and glucose was injected intraperitoneally at a dose of 1 g/kg. (n = 6-8 per group). (C) The IPITT was performed on 9-week-old mice. Mice were fasted for 6 h and then the blood glucose levels were measured and glucose disposal was calculated at the indicated time points before and after intraperitoneal injections of insulin (0.75 U/kg) (n = 6-8 per group). All data are presented as the mean ± sem, *$P < 0.05$, **$P < 0.01$. (D, E) Oxygen consumption (VO$_2$, left), carbon dioxide generation (VCO$_2$, right) and energy expenditure (EE, E) of 9-week-old *ob/ob* mice treated with or without LY2405319. Mice were analyzed by indirect calorimetry over a period of one 12 h light/12 h dark cycle (n = 5 per group). The data are presented as the mean ± sem, **$P < 0.01$.

group (**Figure 1C**). These data show that the administration of LY2405139 alleviated hepatic steatosis in *ob/ob* mice.

LY2405319 prevented oxidative stress and lipid peroxidation in the livers of the ob/ob mice

Oxidative stress plays a central role in the pathophysiology of NAFLD as well as type 2 diabetes [25]. We performed immunohistochemical staining of 8-hydroxy-2'-deoxyguanosine (8-OHdG), a predominant form of free radical-induced oxidative lesion, to evaluate the effect of LY2405139 on oxidative stress in the livers of *ob/ob* mice [26]. Consistent with previous studies, the number of 8-OHdG-positive hepatocytes in vehicle-treated *ob/ob* mice was greater that of than *ob/+*mice. However, the LY2405319 treatment reduced the number of 8-OHdG-positive hepatocytes (*ob/+*control mice, 1.1 ± 0.9%; *ob/ob*-vehicle mice, 32 ± 8.3%; *ob/ob*-LY mice, 9.4 ± 4.3%) (**Figure 2A** and **2B**).

An increase in the reactive oxygen species levels in cells engorged with fat enhances lipid peroxidation. Therefore, we performed the

TBARS assay to measure lipid peroxidation in the livers of these mice [27]. The TBARS levels were elevated in the livers of vehicle-treated *ob/ob* mice compared with *ob/+*mice. However, the livers of LY240319-treated *ob/ob* mice showed significantly reduced TBARS levels (*ob/+*control mice, 0.4 ± 0.3 nmol/mg; *ob/ob*-vehicle mice, 1.4 ± 0.8 nmol/mg; *ob/ob*-LY mice, 0.8 ± 0.2 nmol/mg) (**Figure 2C**). These data indicate that the LY240319 treatment prevented oxidative damage and hepatic lipid peroxidation.

LY2405319 reduced inflammatory signaling in the livers of ob/ob mice

Inflammation is also a critical factor in the progression from hepatic steatosis to steatohepatitis. The inflammatory process is provoked by the activation of various kinases, such as NF-kB, p38 mitogen-activated protein kinases (MAPK), and c-Jun N-terminal kinases (JNKs). NF-kB, p38 MAPK and JNK phosphorylation were observed by western blot analysis to determine the effect of LY2405319 on inflammatory signaling. The levels of phosphorylated NF-κB

p65 were upregulated in the livers of vehicle-treated *ob/ob* mice compared with *ob/+*mice. In addition, the levels of phosphorylated p38 and JNK 1/2 were also elevated. However, the LY2405319 treatment resulted in a significant decrease in the phosphorylation of NF-κB p65, p38 and JNK 1/2 (**Figure 3A**). These data suggest that LY2405319 inhibited NAFLD-related inflammatory signaling.

TNF-α is a key inflammatory mediator of the pathogenesis of NAFLD [28]. The livers of vehicle-treated *ob/ob* mice exhibited a significant increase in TNF-α mRNA expression compared with *ob/+*mice; however, the LY2405319 treatment inhibited TNF-α mRNA expression in the liver. Hepatic TNF-α secretion was decreased in LY2405319-treated animals, as confirmed by ELISA (**Figure 3B**). The proinflammatory cytokine TNF-α amplifies local immune responses by recruiting macrophages. Consequently, increased F4/80 reactivity, an antibody that detects macrophages, was observed in the livers of vehicle-treated *ob/ob* mice; however, the LY2405319 treatment reduced F4/80 reactivity in the livers of *ob/ob* mice (**Figure 3C**). These results indicate that LY2405319 attenuated inflammatory signaling and macrophage infiltration in the livers of *ob/ob* mice.

LY2405319 prevented weight gain, improved insulin sensitivity and increased energy expenditure in ob/ob mice

Fibroblast growth factor 21 is known to affect systemic metabolism and NAFLD. Accordingly, we assessed the systemic effects of LY2405319 on body weight, glucose homeostasis and energy expenditure. **Figure 4A** shows the representative body weights of *ob/ob* mice that were treated with vehicle or LY2405319. Consistent with previous studies using recombinant FGF21 [13], the LY2405319 treatment reduced the body weights of *ob/ob* mice by 21 ± 3.7% after the 3-week treatment compared to the vehicle-treated controls (**Figure 4A**). An intraperitoneal glucose tolerance test and insulin tolerance test were performed after the 3-week LY2405319 or vehicle treatment. The fasting glucose concentration was not different between the vehicle and LY2405319 treatment groups. However, the glucose excursion after glucose challenge was improved by the LY2405319 treatment (**Figure 4B**). The insulin-mediated glucose disposal was also significantly increased by the LY2405319 treatment (**Figure 4C**).

We used indirect calorimetry to calculate energy expenditure and substrate oxidation by measuring O_2 consumption (VO_2) and CO_2 production (VOC_2) after LY2405319 or vehicle treatment to clarify the effects of LY2405319 on energy metabolism. We detected a significant increase in O_2 consumption and CO_2 production in *ob/ob* mice that were treated with LY2405319 (**Figure 4D**). Energy expenditure was increased in LY2405319-treated *ob/ob* mice during both the day and night periods (*ob/ob*-vehicle mice during day, 3200 ± 180 kcal/day/kg^{-1}; *ob/ob*-LY mice during day, 5400 ± 470 kcal/day/kg^{-1}; *ob/ob*-vehicle mice during night, 3700 ± 260 kcal/day/kg^{-1}; *ob/ob*-LY mice during night, 6100 ± 480 kcal/day/kg^{-1}) (**Figure 4E**). Therefore, the LY2405319 treatment prevented weight gain, improved insulin sensitivity, and increased energy expenditure.

LY2405319 improved mitochondrial function by increasing the OCR and beta-oxidation

Decreased oxidative capacity and mitochondrial aberrations are known to be major contributors to the development of insulin resistance and accumulation of fatty acids in nonadipose tissues [29]. Accumulating and emerging evidence also indicates that hepatic mitochondria play a critical role in the development and pathogenesis of NAFLD [30]. Therefore, we analyzed the effects of LY2405319 on mitochondrial beta-oxidation. Primary hepatocytes isolated from the livers of WT mice were treated with LY2405319 or vehicle and the OCR was measured. The results indicate that LY2405319 increased the OCR in a dose-dependent manner (**Figure 5A**). We treated primary hepatocytes with palmitate-BSA and LY2405319 or vehicle to measure fatty acid oxidation. The addition of palmitate-BSA resulted in a dose-dependent increase in the OCR in the LY2405319-treated primary hepatocytes (**Figure 5B**). Therefore, LY2405319 increased the oxidative capacity and fatty acid oxidation, indicating that mitochondrial function was improved. Consistent with these *in vitro* studies, the expression of peroxisome proliferator-activated receptor-γ coactiveator-1 α (Pgc-1α), a transcriptional coactivator that is a central inducer of mitochondrial biogenesis, was upregulated in LY2403519-treated *ob/ob* mice. In addition, the expression of genes involved in electron transport chain complexes, such as Ndufa9, Cox1, and Atpase, was increased in the
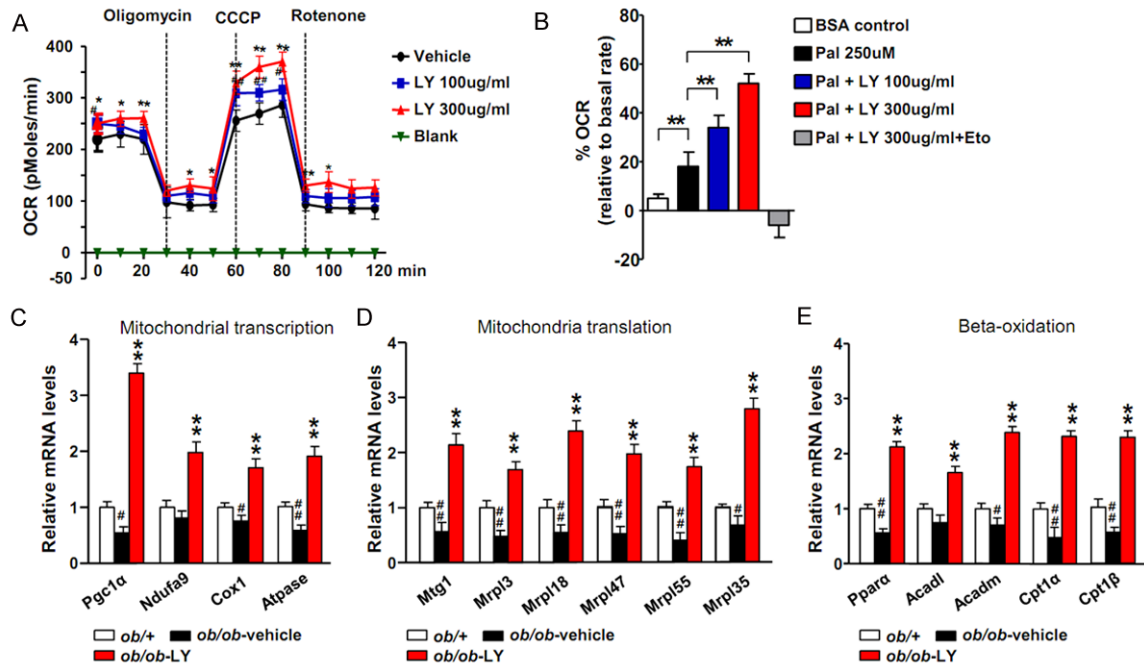
Figure 5. LY2405319 improves mitochondrial function by increasing the OCR and beta-oxidation. (A) OCR measured in primary cultured hepatocytes treated with the indicated concentrations of LY2405319. *P < 0.05, **P < 0.01. Vehicle vs. LY2405319 (B) Fatty acid oxidation in primary hepatocytes using palmitate-BSA as substrate after pre-treatment with different concentrations of LY2405319 in the absence or presence of the CPT1 inhibitor, etomoxir (at 40 μM). (C-E) Expression of genes related to mitochondrial transcription (Pgc1α, Ndufa9, Cox1 and Atpase), mitochondrial translation (Mtg1, Mrpl3, Mrpl18, Mrpl47, Mrpl55 and Mrpl35) and beta-oxidation (Pparα, Acadl, Acadm, Cat1α and Cpt1β) in the livers of ob/ob-vehicle and ob/ob-LY2403519 mice (n = 6 per group). The data are presented as the mean ± sem. #P < 0.05, ##P < 0.01. ob/+vs. ob/ob-vehicle; *P < 0.05, **P < 0.01. ob/ob-vehicle vs. ob/ob-LY2405319.

qRT-PCR analysis. The expression of mitochondrial ribosomal proteins related to mitochondrial translation (Mtg1, Mrpl3, Mrpl18, Mrpl47, Mrpl55, Mrpl35) was also upregulated. Furthermore, the expression of both carnitine palmitoyltransferase 1 (CPT1), the primary rate-controlling enzyme in fatty acid oxidation, and other beta-oxidation controlling genes, such as Pparα, Acadl, and Acadm, were increased by the LY2403519 treatment *in vivo* (**Figure 5C-E**). Taken together, the data indicate that LY2405319 increased both mitochondrial biogenesis and beta-oxidation, thus restoring mitochondrial function.

LY2405319 inhibited liver fibrosis in MCD-fed ob/ob mice

Ob/ob mice possess a spontaneous mutation in the *leptin* gene and are protected against fibrosis and thus fail to progress from steatosis to the more severe steatohepatitis. Secondary insults, such as an MCD diet, are needed to trigger steatohepatitis in *ob/ob* mice and circum-

vent this limitation [31]. We fed 6-week-old *ob/ob* mice an MCD diet for 4 weeks to clarify whether LY2405319 reversed steatohepatitis. As shown in **Figure 6A**, Masson's trichrome staining showed the development of pericellular fibrosis in MCD diet-fed mice. In contrast, when the fibrotic mice were treated with LY2405319, the intensity of Masson's trichrome staining was significantly reduced compared with vehicle-treated mice. The expression of both the type-1a collagen and TGF-β mRNAs was also significantly decreased by the LY2405319 treatment (**Figure 6B**).

The serum AST and ALT levels were significantly increased in MCD-fed *ob/ob* mice, but the LY2405319 treatment decreased the serum levels of these liver injury markers (**Figure 6C**). In addition, MCD-fed *ob/ob* mice that were treated with LY2405319 exhibited an approximately 50% decrease in the hepatic TG and cholesterol levels (**Figure 6D**). In the western blot assay, MCD-fed *ob/ob* mice showed a significant increase in NF-kB p65, JNK 1/2 and
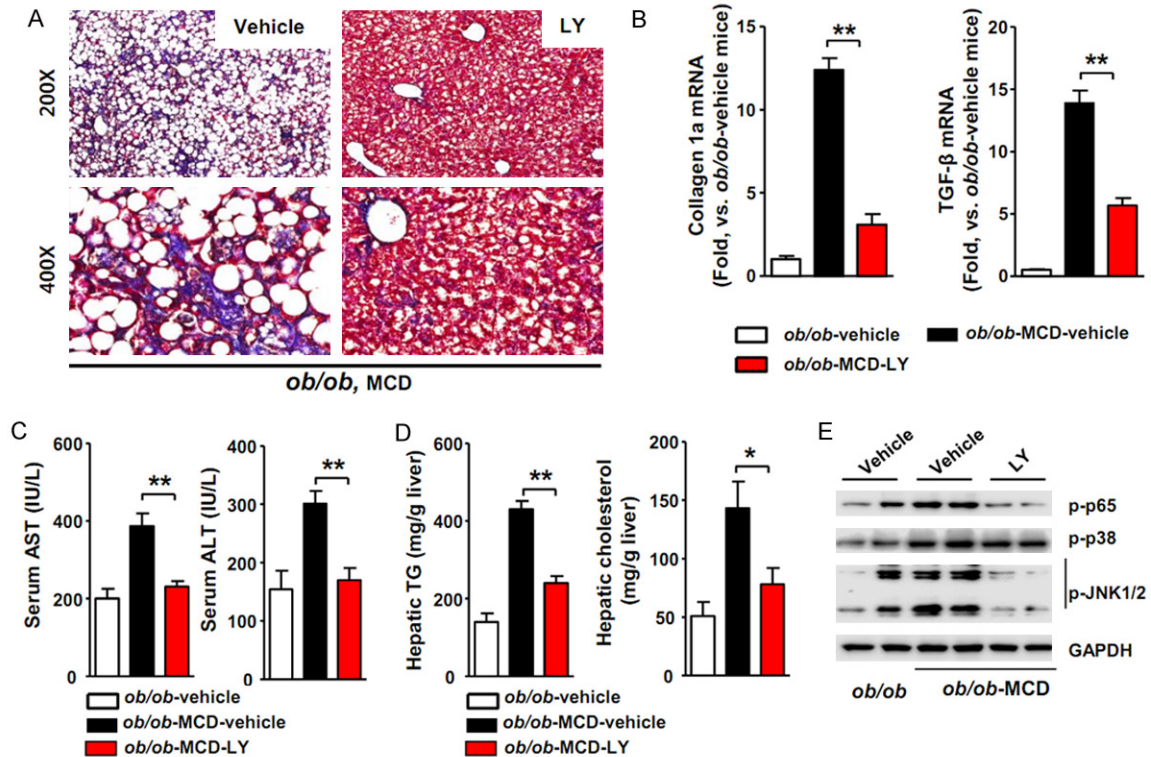
Figure 6. LY2405319 inhibits liver fibrosis in MCD diet-fed *ob/ob* mice. (A) Representative photomicrographs showing the effect of the MCD diet on collagen deposition in MCD-vehicle-fed and MCD-LY2405319-fed *ob/ob* mice. Paraffin-embedded sections from MCD-vehicle-fed *ob/ob* and MCD-LY2405319-fed *ob/ob* mice were stained with Masson's trichrome stain. The arrows indicate pericellular fibrosis in MCD-vehicle-fed *ob/ob* mice (n = 10 per group). (B) Analysis of collagen type-1α and TGF-β1 mRNA expression by qRT-PCR. **P < 0.01 (C) Serum AST and ALT levels in MCD-vehicle-fed or MCD-LY2405319-fed *ob/ob* mice. **P < 0.01 Vehicle vs. LY2405319 (n = 6-8 per group). (D) Hepatic TG and cholesterol levels in MCD-vehicle-fed or MCD-LY2405319-fed *ob/ob* mice (n = 6-8 per group). *P < 0.05, **P < 0.01. (E) Effect of LY2405319 on inflammatory signaling in the livers of the MCD diet-fed *ob/ob* mice treated with or without LY2405319. Western blot analyses of liver extracts were performed to detect NF-kB p65, p38 and JNK 1/2 phosphorylation. GAPDH was used as a loading control. The blots are representative of three independent experiments.

p38 phosphorylation compared with *ob/ob* mice that were fed a normal chow diet. However, the LY2405319 treatment inhibited the phosphorylation of these inflammatory markers in the livers of MCD-fed *ob/ob* mice (**Figure 6E**). Collectively, these data show that the MCD diet amplified inflammatory signaling and liver fibrosis in vehicle-treated *ob/ob* mice, whereas the LY2405319 treatment reversed the progression of NASH and its related pathogenesis. Hence, we propose that LY2405319 is a potentially effective therapeutic candidate for the treatment of NASH.

Discussion

According to the hypothesis for the development of NAFLD, impaired oxidative phosphorylation and increased ROS generation play a central role in the pathophysiology of NASH. Mitochondrial dysfunction contributes to the pathogenesis of NAFLD because it affects hepatic lipid homeostasis and promotes ROS production, lipid peroxidation, cytokine release, and cell death [32]. Indeed, mitochondrial respiratory chain activity is decreased in patients with NASH and in ob/ob mice with NAFLD [33, 34]. Rector et al. also showed that mitochondrial dysfunction precedes both insulin resistance and hepatic steatosis and consequently contributes to the natural history of NAFLD in an obese rodent model [35]. Metformin and thiazolidinedione, available drugs with proven modest benefits for NAFLD, also increase mitochondrial fatty acid oxidation by activating 5'-adenosine monophosphate (AMP)-activated protein kinase [36-40]. In our study, LY2405319 upregulated the expression of

mitochondrial transcription-, translation- and beta-oxidation related genes; increased OCR and fatty acid oxidation; and subsequently decreased oxidative stress and lipid peroxidation. Therefore, LY2405319 could be an effective therapeutic drug for NASH by modulating its diverse pathogenesis in the "multi-hit" model, namely, lipotoxicity, oxidative stress, chronic inflammatory stress and mitochondrial dysfunction.The metabolic effects of exogenously administered FGF21 have been thought to be mediated by the white adipose tissue through increased browning, energy expenditure and glucose disposal. In our study, chronic administration of an FGF21 variant also increased energy expenditure, prevented weight gain and improved insulin sensitivity, as expected (**Figure 4**). Therefore, we must also consider that the systemic effect of LY2405319, an FGF21 variant, resulted in the reversal of NAFLD. However, there are several lines of evidence that highlight the liver as a key site of action for the metabolic effects of FGF21. Zhang et al. showed that the overexpression of FGF21 repressed the transcription of sterol regulatory element binding protein 1c, the gene required for de novo lipogenesis in human liver-derived HepG2 cells [41]. In addition, decreased expression of Pparα was also reported in hepatocytes transfected with an FGF21 siRNA [42]. In addition, FGF21 activates AMP-activated protein kinase and sirtuin 1 and deacetylates its downstream target, Pgc-1α, in adipocytes [43]. In our study, the expression of both Pparα and Pgc-1α was upregulated in LY2405319-treated *ob/ob* mice. Moreover, we showed a dose-dependent increase in the OCR and fatty acid oxidation in LY2405319-treated primary hepatocytes obtained from *ob/ob* mice (**Figure 5**). Therefore, we suggest that LY2405319 suppress hepatic lipogenesis, increases lipolysis, and subsequently increases fatty acid metabolism in the mitochondria. In addition, LY2405319 also improved mitochondrial function; therefore, mitochondria could handle the increased fatty acids without producing more ROS in the liver. Consequently, we showed the direct effect of LY2405319 on the liver, in addition to its systemic effects, particularly on the adipose tissue. Furthermore, we should consider that the NAFLD-associated hepatic insulin resistance could be a cause or precursor of the metabolic syndrome [44]. FGF21 administration was shown to improve hepatic insulin resistance [45]. Inflammation is a required

pathological feature that defines NASH. Compared to simple steatosis, NASH is a significant risk factor for hepatic cirrhosis and hepatocellular carcinoma. Therefore, the therapeutic drugs for NAFLD must also reverse the inflammation in the liver. As shown in **Figure 3**, LY2405319 decreased the hepatic levels of TNF-α, a proinflammatory cytokine secreted by injured hepatocytes. It also decreased the phosphorylation of NF-kB, p38 MAPK and JNK, the main inflammatory signaling pathways that are activated by proinflammatory cytokines, such as TNF-α. In addition, the histological manifestations of inflammation were also decreased in the livers of LY2405319-treated *ob/ob* mice. Moreover, LY2405319 reversed MCD diet-induced hepatic fibrosis in both histology with Masson's trichrome staining and the expression of fibrosis marker genes (**Figure 6**). Collectively, LY2405319 reversed all of the main pathological consequences of NASH, namely, hepatic steatosis, inflammation, and fibrosis. Accordingly, LY2405319 showed good potential as an effective therapeutic drug for the treatment of NASH.

Several experimental studies of native FGF21 or FGF21 analogues have implicated FGF21 in the treatment of NAFLD. Intraperitoneal administration of 10 mg/kg recombinant murine FGF21 for 6 weeks reversed hepatic steatosis in diet-induced obese mice, as determined by histological examinations of liver sections and biochemical analyses of the hepatic TG and cholesterol content [13]. ob/ob mice that received 1 mg/kg recombinant human FGF21 for 2 weeks via continuous subcutaneous administration exhibited a decreased liver weight, without histological examination or biochemical analyses of the liver [14]. A polyethylene glycol-conjugated FGF21 developed with the aim of extending the half-life of FGF21 also reduced the hepatic TG levels in db/db mice that were subcutaneously injected for 12 days [46]. However, these studies did not show the effect of FGF21 on hepatic inflammation and fibrosis; therefore, they could not confirm the therapeutic effect on NASH. We showed that the FGF21 variant LY2405319 reversed hepatic steatosis, inflammation and fibrosis in *ob/ob* mice. Although *ob/ob* mice are not an ideal animal model in which to study inflammation and fibrosis in NASH because of their own characteristics, including leptin deficiency, they exhibited hepatic lipid accumulation, oxidative stress

and mitochondrial dysfunction [24]. Furthermore, the MCD diet increased oxidative stress to progress them to a stage of the disease that resembles classical NASH features [31].

In conclusion, our study showed that the therapeutic effects of LY2405319 on NASH were to reduce inflammation and reverse fibrosis in the liver, as well as to improve hepatic steatosis. Additional studies may be required in other well-established liver models, such as diet-induced obese rodents, to solidify the beneficial effects of LY2405319 on NASH. Furthermore, we found that LY2405319 restored mitochondrial function, which could be a mechanism by which LY2405319 exerted its therapeutic effects on the liver, as well as its systemic effects.

Acknowledgements

Disclosure of conflict of interest

None.

Address correspondence to: Hyo Kyun Chung and Koon Soon Kim, Research Center for Endocrine and Metabolic Diseases, Chungnam National University School of Medicine, Daejeon 35015, Republic of Korea. Tel: +82-42-280-6800; Fax: +82-42-280-6990; E-mail: hkchung74@cnu.ac.kr (HKC); Tel: +82-42-280-7134; Fax: 82-42-280-6990; E-mail: kunsunkim@cnu.ac.kr (KSK)

References

[1] Williams CD, Stengel J, Asike MI, Torres DM, Shaw J, Contreras M, Landt CL and Harrison SA. Prevalence of nonalcoholic fatty liver disease and nonalcoholic steatohepatitis among a largely middle-aged population utilizing ultrasound and liver biopsy: a prospective study. Gastroenterology 2011; 140: 124-131.

[2] Rinella ME. Nonalcoholic fatty liver disease: a systematic review. JAMA 2015; 313: 2263-2273.

[3] Matteoni CA, Younossi ZM, Gramlich T, Boparai N, Liu YC and McCullough AJ. Nonalcoholic fatty liver disease: a spectrum of clinical and pathological severity. Gastroenterology 1999; 116: 1413-1419.

[4] Adams LA, Lymp JF, St Sauver J, Sanderson SO, Lindor KD, Feldstein A and Angulo P. The natural history of nonalcoholic fatty liver disease: a population-based cohort study. Gastroenterology 2005; 129: 113-121.

[5] Adams LA, Sanderson S, Lindor KD and Angulo P. The histological course of nonalcoholic fatty liver disease: a longitudinal study of 103 patients with sequential liver biopsies. J Hepatol 2005; 42: 132-138.

[6] Tilg H and Moschen AR. Evolution of inflammation in nonalcoholic fatty liver disease: the multiple parallel hits hypothesis. Hepatology 2010; 52: 1836-1846.

[7] Yao HR, Liu J, Plumeri D, Cao YB, He T, Lin L, Li Y, Jiang YY, Li J and Shang J. Lipotoxicity in HepG2 cells triggered by free fatty acids. Am J Transl Res 2011; 3: 284-291.

[8] Utzschneider KM and Kahn SE. Review: The role of insulin resistance in nonalcoholic fatty liver disease. J Clin Endocrinol Metab 2006; 91: 4753-4761.

[9] Birkenfeld AL and Shulman GI. Nonalcoholic fatty liver disease, hepatic insulin resistance, and type 2 diabetes. Hepatology 2014; 59: 713-723.

[10] Li H, Zhang J and Jia W. Fibroblast growth factor 21: a novel metabolic regulator from pharmacology to physiology. Front Med 2013; 7: 25-30.

[11] Inagaki T, Dutchak P, Zhao G, Ding X, Gautron L, Parameswara V, Li Y, Goetz R, Mohammadi M, Esser V, Elmquist JK, Gerard RD, Burgess SC, Hammer RE, Mangelsdorf DJ and Kliewer SA. Endocrine Regulation of the Fasting Response by PPARα-Mediated Induction of Fibroblast Growth Factor 21. Cell Metabolism 2007; 5: 415-425.

[12] Dutchak Paul A, Katafuchi T, Bookout Angie L, Choi Jang H, Yu Ruth T, Mangelsdorf David J and Kliewer Steven A. Fibroblast Growth Factor-21 Regulates PPARγ Activity and the Antidiabetic Actions of Thiazolidinediones. Cell 2012; 148: 556-567.

[13] Xu J, Lloyd DJ, Hale C, Stanislaus S, Chen M, Sivits G, Vonderfecht S, Hecht R, Li YS, Lindberg RA, Chen JL, Jung DY, Zhang Z, Ko HJ, Kim JK and Veniant MM. Fibroblast growth factor 21 reverses hepatic steatosis, increases energy expenditure, and improves insulin sensitivity in diet-induced obese mice. Diabetes 2009; 58: 250-259.

[14] Coskun T, Bina HA, Schneider MA, Dunbar JD, Hu CC, Chen Y, Moller DE and Kharitonenkov A.

Fibroblast Growth Factor 21 Corrects Obesity in Mice. Endocrinology 2008; 149: 6018-6027.

[15] Kharitonenkov A, Shiyanova TL, Koester A, Ford AM, Micanovic R, Galbreath EJ, Sandusky GE, Hammond LJ, Moyers JS, Owens RA, Gromada J, Brozinick JT, Hawkins ED, Wroblewski VJ, Li DS, Mehrbod F, Jaskunas SR and Shanafelt AB. FGF-21 as a novel metabolic regulator. J Clin Invest 2005; 115: 1627-1635.

[16] Kharitonenkov A, Wroblewski VJ, Koester A, Chen YF, Clutinger CK, Tigno XT, Hansen BC, Shanafelt AB and Etgen GJ. The Metabolic State of Diabetic Monkeys Is Regulated by Fibroblast Growth Factor-21. Endocrinology 2007; 148: 774-781.

[17] Gaich G, Chien JY, Fu H, Glass LC, Deeg MA, Holland WL, Kharitonenkov A, Bumol T, Schilske HK and Moller DE. The effects of LY2405319, an FGF21 analog, in obese human subjects with type 2 diabetes. Cell Metab 2013; 18: 333-340.

[18] Liu J, Xu Y, Hu Y and Wang G. The role of fibroblast growth factor 21 in the pathogenesis of non-alcoholic fatty liver disease and implications for therapy. Metabolism 2015; 64: 380-390.

[19] Adams AC, Yang C, Coskun T, Cheng CC, Gimeno RE, Luo Y and Kharitonenkov A. The breadth of FGF21's metabolic actions are governed by FGFR1 in adipose tissue. Mol Metab 2012; 2: 31-37.

[20] Fisher FM, Estall JL, Adams AC, Antonellis PJ, Bina HA, Flier JS, Kharitonenkov A, Spiegelman BM and Maratos-Flier E. Integrated regulation of hepatic metabolism by fibroblast growth factor 21 (FGF21) in vivo. Endocrinology 2011; 152: 2996-3004.

[21] Zhang J and Li Y. Fibroblast growth factor 21, the endocrine FGF pathway and novel treatments for metabolic syndrome. Drug Discov Today 2014; 19: 579-589.

[22] Kharitonenkov A, Beals JM, Micanovic R, Strifler BA, Rathnachalam R, Wroblewski VJ, Li S, Koester A, Ford AM, Coskun T, Dunbar JD, Cheng CC, Frye CC, Bumol TF and Moller DE. Rational design of a fibroblast growth factor 21-based clinical candidate, LY2405319. PLoS One 2013; 8: e58575.

[23] Ryu MJ, Kim SJ, Kim YK, Choi MJ, Tadi S, Lee MH, Lee SE, Chung HK, Jung SB, Kim HJ, Jo YS, Kim KS, Lee SH, Kim JM, Kweon GR, Park KC, Lee JU, Kong YY, Lee CH, Chung J and Shong M. Crif1 deficiency reduces adipose OXPHOS capacity and triggers inflammation and insulin resistance in mice. PLoS Genet 2013; 9: e1003356.

[24] Chung HK, Kim YK, Park JH, Ryu MJ, Chang JY, Hwang JH, Lee CH, Kim SH, Kim HJ, Kweon GR, Kim KS and Shong M. The indole derivative

NecroX-7 improves nonalcoholic steatohepatitis in ob/ob mice through suppression of mitochondrial ROS/RNS and inflammation. Liver Int 2015; 35: 1341-1353.

[25] Chang YC and Chuang LM. The role of oxidative stress in the pathogenesis of type 2 diabetes: from molecular mechanism to clinical implication. Am J Transl Res 2010; 2: 316-331.

[26] Cheng KC, Cahill DS, Kasai H, Nishimura S and Loeb LA. 8-Hydroxyguanine, an abundant form of oxidative DNA damage, causes G----T and A----C substitutions. J Biol Chem 1992; 267: 166-172.

[27] Janero DR. Malondialdehyde and thiobarbituric acid-reactivity as diagnostic indices of lipid peroxidation and peroxidative tissue injury. Free Radic Biol Med 1990; 9: 515-540.

[28] Seo YY, Cho YK, Bae JC, Seo MH, Park SE, Rhee EJ, Park CY, Oh KW, Park SW and Lee WY. Tumor Necrosis Factor-alpha as a Predictor for the Development of Nonalcoholic Fatty Liver Disease: A 4-Year Follow-Up Study. Endocrinol Metab (Seoul) 2013; 28: 41-45.

[29] Schrauwen P and Hesselink MK. Oxidative capacity, lipotoxicity, and mitochondrial damage in type 2 diabetes. Diabetes 2004; 53: 1412-1417.

[30] Nassir F and Ibdah JA. Role of Mitochondria in Nonalcoholic Fatty Liver Disease. Int J Mol Sci 2014; 15: 8713-8742.

[31] Takahashi Y, Soejima Y and Fukusato T. Animal models of nonalcoholic fatty liver disease/nonalcoholic steatohepatitis. World J Gastroenterol 2012; 18: 2300-2308.

[32] Begriche K, Igoudjil A, Pessayre D and Fromenty B. Mitochondrial dysfunction in NASH: causes, consequences and possible means to prevent it. Mitochondrion 2006; 6: 1-28.

[33] Perez-Carreras M, Del Hoyo P, Martin MA, Rubio JC, Martin A, Castellano G, Colina F, Arenas J and Solis-Herruzo JA. Defective hepatic mitochondrial respiratory chain in patients with nonalcoholic steatohepatitis. Hepatology 2003; 38: 999-1007.

[34] Garcia-Ruiz I, Rodriguez-Juan C, Diaz-Sanjuan T, del Hoyo P, Colina F, Munoz-Yague T and Solis-Herruzo JA. Uric acid and anti-TNF antibody improve mitochondrial dysfunction in ob/ob mice. Hepatology 2006; 44: 581-591.

[35] Rector RS, Thyfault JP, Uptergrove GM, Morris EM, Naples SP, Borengasser SJ, Mikus CR, Laye MJ, Laughlin MH, Booth FW and Ibdah JA. Mitochondrial dysfunction precedes insulin resistance and hepatic steatosis and contributes to the natural history of non-alcoholic fatty liver disease in an obese rodent model. J Hepatol 2010; 52: 727-736.

[36] Lin HZ, Yang SQ, Chuckaree C, Kuhajda F, Ronnet G and Diehl AM. Metformin reverses fatty liver disease in obese, leptin-deficient mice. Nat Med 2000; 6: 998-1003.

[37] Marchesini G, Brizi M, Bianchi G, Tomassetti S, Zoli M and Melchionda N. Metformin in non-alcoholic steatohepatitis. Lancet 2001; 358: 893-894.

[38] Zhou G, Myers R, Li Y, Chen Y, Shen X, Fenyk-Melody J, Wu M, Ventre J, Doebber T, Fujii N, Musi N, Hirshman MF, Goodyear LJ and Moller DE. Role of AMP-activated protein kinase in mechanism of metformin action. J Clin Invest 2001; 108: 1167-1174.

[39] Neuschwander-Tetri BA, Brunt EM, Wehmeier KR, Oliver D and Bacon BR. Improved nonalcoholic steatohepatitis after 48 weeks of treatment with the PPAR-gamma ligand rosiglitazone. Hepatology 2003; 38: 1008-1017.

[40] Saha AK, Avilucea PR, Ye JM, Assifi MM, Kraegen EW and Ruderman NB. Pioglitazone treatment activates AMP-activated protein kinase in rat liver and adipose tissue in vivo. Biochem Biophys Res Commun 2004; 314: 580-585.

[41] Zhang Y, Lei T, Huang JF, Wang SB, Zhou LL, Yang ZQ and Chen XD. The link between fibroblast growth factor 21 and sterol regulatory element binding protein 1c during lipogenesis in hepatocytes. Mol Cell Endocrinol 2011; 342: 41-47.

[42] Lee J, Hong SW, Park SE, Rhee EJ, Park CY, Oh KW, Park SW and Lee WY. Exendin-4 regulates lipid metabolism and fibroblast growth factor 21 in hepatic steatosis. Metabolism 2014; 63: 1041-1048.

[43] Chau MD, Gao J, Yang Q, Wu Z and Gromada J. Fibroblast growth factor 21 regulates energy metabolism by activating the AMPK-SIRT1-PGC-1alpha pathway. Proc Natl Acad Sci U S A 2010; 107: 12553-12558.

[44] Lonardo A, Ballestri S, Marchesini G, Angulo P and Loria P. Nonalcoholic fatty liver disease: a precursor of the metabolic syndrome. Dig Liver Dis 2015; 47: 181-190.

[45] Camporez JP, Jornayvaz FR, Petersen MC, Pesta D, Guigni BA, Serr J, Zhang D, Kahn M, Samuel VT, Jurczak MJ and Shulman GI. Cellular mechanisms by which FGF21 improves insulin sensitivity in male mice. Endocrinology 2013; 154: 3099-3109.

[46] Mu J, Pinkstaff J, Li Z, Skidmore L, Li N, Myler H, Dallas-Yang Q, Putnam AM, Yao J, Bussell S, Wu M, Norman TC, Rodriguez CG, Kimmel B, Metzger JM, Manibusan A, Lee D, Zaller DM, Zhang BB, DiMarchi RD, Berger JP and Axelrod DW. FGF21 analogs of sustained action enabled by orthogonal biosynthesis demonstrate enhanced antidiabetic pharmacology in rodents. Diabetes 2012; 61: 505-512.